

## Article

# Pyrolysis Temperature and Application Rate of Sugarcane Straw Biochar Influence Sorption and Desorption of Metribuzin and Soil Chemical Properties

Kamila C. Mielke <sup>1</sup>, Ana Flávia S. Laube <sup>2</sup>, Tiago Guimarães <sup>2</sup>, Maura Gabriela da S. Brochado <sup>1</sup>, Bruna Aparecida de P. Medeiros <sup>1</sup> and Kassio F. Mendes <sup>1,\*</sup>

<sup>1</sup> Department of Agronomy, Federal University of Viçosa, Viçosa 36.570-900, Brazil

<sup>2</sup> Department of Chemistry, Federal University of Viçosa, Viçosa 36.570-900, Brazil

\* Correspondence: kfmendes@ufv.br

**Abstract:** Pyrolysis temperature and application rate of biochar to soil can influence herbicide behavior and soil fertility. The objective was to investigate the effect of soil amendments with application rates of sugarcane straw biochar, produced at different pyrolysis temperatures, on the sorption–desorption of metribuzin in soil. The analysis was performed using high-performance liquid chromatography (HPLC). The treatments were three pyrolysis temperatures (BC350, BC550 and BC750 °C) and seven application rates (0, 0.1, 0.5, 1, 1.5, 5 and 10% w w<sup>-1</sup>). Amended soil with different application rates decreased H + Al and increased pH, OC, P, K, Ca, Mg, Fe, Mn, CEC and BS contents.  $K_f$  values of sorption and desorption of metribuzin were 1.42 and 0.78 mg<sup>(1-1/n)</sup> L<sup>1/n</sup> Kg<sup>-1</sup>, respectively, in the unamended soil. Application rates < 1% of biochar sorbed ~23% and desorbed ~15% of metribuzin, similar to unamended soil, for all pyrolysis temperatures. Amended soil with 10% of BC350, BC550 and BC750 sorbed 63.8, 75.5 and 89.4% and desorbed 8.3, 5.8 and 3.7% of metribuzin, respectively. High pyrolysis temperature and application rates of sugarcane straw biochar show an ability to immobilize metribuzin and improve soil fertility, which may influence the effectiveness in weed control.

**Keywords:** carbonaceous material; soil fertility; herbicide behavior; residual in soil; environmental contamination



**Citation:** Mielke, K.C.; Laube, A.F.S.; Guimarães, T.; Brochado, M.G.d.S.; Medeiros, B.A.d.P.; Mendes, K.F. Pyrolysis Temperature and Application Rate of Sugarcane Straw Biochar Influence Sorption and Desorption of Metribuzin and Soil Chemical Properties. *Processes* **2022**, *10*, 1924. <https://doi.org/10.3390/pr10101924>

Academic Editor: Carmen Branca

Received: 25 August 2022

Accepted: 17 September 2022

Published: 23 September 2022

**Publisher's Note:** MDPI stays neutral with regard to jurisdictional claims in published maps and institutional affiliations.



**Copyright:** © 2022 by the authors. Licensee MDPI, Basel, Switzerland. This article is an open access article distributed under the terms and conditions of the Creative Commons Attribution (CC BY) license (<https://creativecommons.org/licenses/by/4.0/>).

## 1. Introduction

Biochar (BC) is defined as a carbon-rich product, produced by thermal conversion of organic material, with limited oxygen (O<sub>2</sub>) supply and controlled temperatures, consisting mainly of carbon (C) and a variable proportion of oxygen (O) and hydrogen (H) [1]. BC has been used for many years as a corrective in general soil applications. BC has been shown to increase porosity, specific surface area (SSA), soil water holding capacity [2,3], availability of basic cations (Ca<sup>2+</sup>, Mg<sup>2+</sup>, K<sup>+</sup>) [4,5], increased pH and cation exchange capacity (CEC) [3], in addition to its significant content of recalcitrant C that offers the possibility of long-term C sequestration [6]. Corn residue BC produced at different pyrolysis temperatures was added to two different soils [7]. These authors observed that increasing the pyrolysis temperature of biochar added to sandy loam soil improved the pH (0.46 units), electrical conductivity (EC) (0.38 dS m<sup>-1</sup>), N (120%) and K (41%), but decreased plant-available P (−86%), relative to unamended soil. Differently, a corn BC produced at a pyrolysis temperature of 200 °C and applied at a rate of 2% (w w<sup>-1</sup>) in calcareous soil was more efficient in the availability of nutrients to the soil [8]. The effects on soil fertility and consequently on crop productivity are related to the physicochemical properties of soil, biochar, application rates and pyrolysis temperature of biochar production, which can provide different results in soil fertility [9].

Over the years, biochar has also proven to be a material capable of removing pollutants (herbicides, fungicides, insecticides, heavy metals, antibiotics, industrial chemicals, among

others) from soil and water through sorption–desorption and degradation processes [10]. The distinct characteristics of biochar related to surface chemistry (surface functional groups and cation exchange) and morphological structure (e.g., high SSA and microporosity) [11] enables biochar to have high sorptive capacity. The variability in the physical and chemical properties of biochar depends on the raw material and the conditions used during the pyrolysis process [1].

The potential to sorb herbicides in soil has been evidenced by different authors [12–16]. The high sorption of the herbicide in the biochar-amended soil generally decreases its bioavailability for uptake by plants, degradation by microorganisms and leaching into the soil profile [17]. As opposed to the sorption, there is usually a decrease in the desorption of the herbicide and, in some cases, it may become irreversible [18]. The increased sorption of herbicides by biochar decreases their loss through dissipation into the environment, decreasing the risk of human exposure and environmental pollution. However, it can have a high sorption capacity for residual herbicide-applied PRE emergence (directly to the soil), such as metribuzin and reduce the residual effect on weed control.

The metribuzin [4-amino-6-tert-butyl-4,5-dihydro-3-methylthio-1,2,4-triazin-5-one] belongs to the triazinone chemical group and acts in the inhibition of photosystem II (PSII), in the photochemical phase of photosynthesis [19]. The characteristics of high solubility ( $S_w = 10,700 \text{ mg L}^{-1}$  at  $20^\circ\text{C}$ ), high mobility in soil (sorption coefficient normalized by organic carbon content =  $K_{oc}$  of  $38 \text{ mg L}^{-1}$ ), high leaching capacity (GUS index-Groundwater Ubiquity Score = 2.96) and low persistence (half-life degradation time,  $DT_{50} = \sim 20 \text{ d}$ ) [20–22], make the herbicide a product with potential for environmental contamination. Metribuzin was frequently detected at a maximum concentration of  $0.351 \text{ } \mu\text{g L}^{-1}$  in surface and groundwater in untreated human consumption sites in the region of Primavera do Leste, Mato Grosso (Midwestern Brazil) [23]. Metribuzin application contaminated groundwater with its metabolites when applied to sandy soil in Denmark [24]. The authors detected diketometribuzin and desaminodiketometribuzin in soil samples at concentrations exceeding the maximum residue limit set by the European Union ( $0.1 \text{ } \mu\text{g L}^{-1}$ ).

The behavior of metribuzin in biochar-amended soils brought positive results for immobilization and decreased leaching [25–27]. However, the sorption–desorption results are distinct among authors and depend on the temperature in the pyrolysis process, soil application rate and feedstock used. Feedstocks with lower presence of lignin and cellulose (vegetable wastes) produce biochar with low bulk density, high pH and lower C stability than feedstocks with high lignin and cellulose content (wood) [28,29]. Higher pyrolysis temperatures, in general, increase the sorptive capacity of biochar [30]. The use of biochar in agriculture has usually been reported as a soil conditioner and can contribute to the lasting improvement in the chemical, physical, hydric and biological attributes of the soil. The addition of high application rates of biochar can directly interfere in the sorption and desorption of the herbicide-applied pre-emergence directly to the soil. The application of biochar must be carefully determined for its remediation and soil conditioning potential, since increased sorption can lead to decreased efficacy of PRE herbicides, decreasing their residual action.

The objective of this study was to investigate the effect of soil amendments with application rates of sugarcane straw biochar produced at different pyrolysis temperatures on the sorption–desorption processes of metribuzin in soil. The results of this study will determine the best pyrolysis temperature and application rate of sugarcane straw biochar to immobilize metribuzin, thus, reducing its leaching potential into the soil profile. It also seeks to determine, based on the sorptive capacity of biochar, the application rates that will positively influence the chemical attributes of the soil.

## 2. Materials and Methods

### 2.1. Sugarcane Straw Biochar

Sugarcane (*Saccharum officinarum*) straw waste was used as a source of raw material because it is a promising alternative for biochar production [31,32]. Straw is a residue from the mechanical harvesting of sugarcane, grown in abundance in Brazil. The sugarcane straw was crushed, sieved (mesh size 10 mesh, <2.0 mm) and dried in an oven with forced air circulation at  $103 \pm 2$  °C. The straw was placed in a sealed reactor to prevent the ingress of O<sub>2</sub>. The reactor furnace was heated at a rate of  $5$  °C min<sup>-1</sup>, in slow pyrolysis (4–6 h) at temperatures of 350°, 550° and 750 °C. The elemental composition and ash content of biochar was performed according to EPA 3051A [33]. The content of C, N and the C/N ratio was determined by combustion using an elemental analyzer (LECO CS-600, Shimadzu, Japan). The pH was determined according to the guidelines of the analytical methods guide for biochar [34], in which 5 g biochar samples were stirred with 50 mL deionized water (1:10 w v<sup>-1</sup>) in a horizontal shaker for 1 h at  $21 \pm 2$  °C. The specific surface area (SSA) was obtained using the N<sub>2</sub>-Brunauer–Emmett–Teller (BET) method [35] (Table 1).

**Table 1.** Selected properties of sugarcane straw biochar at different pyrolysis temperatures.

T °C	pH	C	N	C/N	Ash	SSA
	H <sub>2</sub> O		%			m <sup>2</sup> g <sup>-1</sup>
350	8.6	48.7	0.832	58.51	5.0	17
550	9.3	49.1	0.647	75.83	10.3	129
750	9.8	59.0	0.403	146.36	11.6	223

Temperature (T); Hydrogen Potential (pH), Carbon (C), Nitrogen (N), Carbon/Nitrogen Ratio (C/N), Specific Surface Area (SSA).

Surface morphology and elemental analysis of biochar were carried out by scanning electron microscopy (SEM) coupled with an X-ray energy dispersive spectrometer (EDS), in an SEM, brand JEOL (JSM-6010LA, Akishima, Tokyo, Japan). This microscope has a resolution of 4 nm (with beam at 20 kV), magnification from 8× to 300,000× and acceleration voltage from 500 V to 20 kV. Also used was an electron gun with pre-centered tungsten filament. Everhart–Thornley detector for secondary electron images and solid-state detector for retro-scattered electrons with contrast of topography, composition and variable shading. Silicon Drift detector for EDS analysis with 133 eV resolution was used. The biochar particles were attached to a metal stub by conductive carbon tape (PELCO Tabs™, Ted Pella, Inc., Redding, CA, USA) and sputter coated (Leica EM ACE 600, Buffalo Grove, IL, USA) with a 120 nm thick layer of gold.

Changes in biochar functional groups were analyzed by Fourier-transform infrared spectroscopy (FTIR), in a Bruker VERTEX 70 instrument (Bruker, Bremen, Germany), using the attenuated total reflectance (ATR) method in a range of 350–4000 cm<sup>-1</sup>. Raman spectroscopy was carried out in a micro-Raman spectrometer (Renishaw InVia, Gloucestershire, England) equipped with an Nd-YAG la ( $\lambda = 514$  nm) and a 50× objective lens (Olympus B × 41) and the Raman spectrum acquisition time for each sample was defined as 10 s.

### 2.2. Soil Collection and Analysis

The agricultural soil samples were collected from the top layer (0–10 cm) in Viçosa, MG, Brazil (20°46′05″ S; 42°52′08″ W), being an area that has not been treated with herbicides for the last three years. The soil samples were air dried for 10 d, then sieved on 5.0 mm mesh and stored at room temperature. The soil was classified as Oxisol (*Latossolo Vermelho-Amarelo*).

The soil was amended with sugarcane straw biochar produced at different pyrolysis temperatures (BC350, BC550 and BC750 °C) in application rates of 0, 0.1, 0.5, 1, 1.5, 5 and 10% (w w<sup>-1</sup>) representing 0, 1, 5, 10, 15, 50 and 100 Mg ha<sup>-1</sup>, respectively, assuming a soil density of 1 g cm<sup>-3</sup> and incorporation depth of 0.10 m. The analyses of P, Na, K, Fe, Zn, Mn and Cu were performed with the Mehlich 1 Extractor. For Ca, Mg and Al the KCl

extractor was used ( $1 \text{ mol L}^{-1}$ ). Potential acidity (H + Al) was extracted in calcium acetate ( $0.5 \text{ mol L}^{-1}$ ) at pH 7.0. For the determination of BS, hot water was used as an extractor and for S, monocalcium phosphate in acetic acid. Organic matter (OM) was quantified by the Walkley-Black titration method after wet oxidation. The conversion of OM into organic carbon (OC) was performed using the correction factor 1.72 (Table 2).

**Table 2.** Physicochemical attributes of the soil amended with sugarcane straw biochar and unamended soil used in this study.

Pyrolysis Temperature	Application Rate	Chemical Attributes													
		pH	OC	P	K	Ca	Mg	H + Al	Zn	Fe	Mn	Cu	B	CEC	BS
(°C)	(%) w w <sup>-1</sup>	H <sub>2</sub> O	%	mg kg <sup>-1</sup>			mmol <sub>c</sub> kg <sup>-1</sup>			mg kg <sup>-1</sup>			mmol <sub>c</sub> kg <sup>-1</sup>	%	
-	unamended	5.5	1.2	1.3	77.0	15.9	5.4	33.0	3.0	129.8	91.0	3.9	0.1	23.3	41.0
350	0.1	5.5	1.2	1.5	97.0	16.0	5.7	33.3	2.9	129.6	99.1	3.8	0.1	24.2	40.0
	0.5	5.5	1.2	2.0	111.0	17.9	6.5	33.0	3.1	123.6	127.0	3.6	0.1	27.8	46.0
	1	5.8	1.2	3.3	125.0	17.5	6.8	26.4	2.8	148.1	130.0	3.7	0.1	29.3	52.0
	1.5	5.9	1.2	6.3	139.0	17.1	7.2	23.1	2.9	154.7	144.0	4.1	0.1	29.4	56.0
	5	6.8	1.2	10.0	240.0	17.7	8.3	13.3	2.9	234.4	155.0	3.8	0.1	36.7	73.0
	10	7.2	1.2	30.0	290.0	17.4	9.6	6.6	2.8	245.5	212.0	3.6	0.1	37.1	85.0
550	0.1	5.4	1.2	2.2	99.0	16.5	5.7	29.4	2.8	128.5	94.5	3.6	0.1	24.7	48.0
	0.5	5.6	1.2	2.7	132.0	16.2	5.8	29.7	3.1	157.4	97.9	4.1	0.1	24.8	45.0
	1	5.8	1.2	4.4	158.0	17.3	6.1	29.7	3.0	228.5	91.2	4.0	0.1	26.6	47.0
	1.5	5.9	1.2	8.7	161.0	17.8	5.8	19.8	2.8	266.5	157.0	3.4	0.1	25.2	56.0
	5	7.0	1.2	15.0	250.0	17.7	7.6	9.9	2.7	273.5	183.0	3.1	0.1	33.2	77.0
	10	7.3	1.3	33.0	340.0	18.1	8.4	3.3	2.9	297.5	202.0	3.6	0.1	38.5	90.0
750	0.1	5.4	1.2	2.9	108.0	16.8	5.6	33.0	2.7	135.0	96.6	3.6	0.1	25.2	43.0
	0.5	5.5	1.2	3.7	144.0	17.4	6.8	29.7	3.0	148.8	135.0	3.9	0.1	27.6	48.0
	1	5.8	1.2	7.8	178.0	17.8	7.0	29.7	2.8	147.6	122.0	4.0	0.1	29.4	49.0
	1.5	6.2	1.2	12.0	240.0	18.1	7.1	13.2	2.5	238.5	123.0	3.8	0.1	30.6	70.0
	5	7.2	1.3	55.0	500.0	19.7	9.8	3.3	2.9	267.5	177.0	3.7	0.1	39.3	92.0
	10	7.6	1.4	65.0	550.0	20.0	11.1	0.0	2.9	294.5	178.0	3.8	0.1	40.6	100.0
Physical Attributes (g kg <sup>-1</sup> )															
Soil	unamended	Sand 500			Silt 120			Clay 380			Texture class sandy clay				

Source: Laboratory of Soil Analysis Viçosa LTDA, Viçosa, MG, Brazil. Hydrogen Potential (pH), Organic Carbon (OC), Phosphorus (P), Potassium (K), Calcium (Ca), Magnesium (Mg), Potential acidity (H + Al), Zinc (Zn), Iron (Fe), Manganese (Mn), Copper (Cu), Boron (B), Cation Exchange Capacity (effective) (CEC), Base Saturation (BS).

### 2.3. Sorption–Desorption Studies

The methodology for the sorption and desorption study was established according to the guidelines “106, Adsorption–Desorption Using a Batch Equilibrium Method” [36,37]. The stock solution was prepared at a concentration of  $500 \text{ mg L}^{-1}$  of the standard Metribuzin-Pestanal™ (Analytical Standard, 98.8% purity Sigma-Aldrich, San Luis, MO, USA) and the working solution at a concentration of  $100 \text{ mg L}^{-1}$ , both in acetonitrile (99.9% purity). From the working solution, five concentrations of metribuzin were prepared in  $0.01 \text{ mol L}^{-1}$   $\text{CaCl}_2$  solution. The concentrations were 0.5, 1, 2, 4 and  $8 \text{ mg L}^{-1}$ , where the concentration of  $2 \text{ mg L}^{-1}$  corresponds to the highest recommended dose of the herbicide ( $1920 \text{ g a.i. ha}^{-1}$ ) for the sugarcane crop, assuming a soil density of  $1 \text{ g cm}^{-3}$  and incorporation depth of 0.10 m.

In Falcon tubes 2 g of soil from each treatment with biochar-amended and unamended soils were added and 10 mL of  $0.01 \text{ mol L}^{-1}$   $\text{CaCl}_2$  solution was added, in triplicate for each treatment. The tubes were then subjected to rotary shaking, using an orbital shaker adapted to a motor (Fisatom 801, São Paulo, Brazil) at 45 rpm for 24 h until they reached the equilibrium concentration [25,26]. Subsequently, the tubes were added to a digital centrifuge (Kasvi, K14-0815P, Paraná, Brazil) at 3500 rpm for 7 min. A 2 mL aliquot was filtered on a Millipore filter (PRFE membrane  $0.45 \mu\text{m}$ ) and placed in a vial. Metribuzin was quantified in a high-performance liquid chromatograph (HPLC) (LC 20AT, Shimadzu, Japan), with photodiode array detector (SPD-M20A, Shimadzu, Japan) and stainless-steel  $\text{C}_{18}$  column (Shimadzu VP-ODS Shim-pack 250 mm  $\times$  4.6 mm d.i.,  $5 \mu\text{m}$  of particle size).

The mobile phase was adapted from [25], composed of acetonitrile/water (acidified with 0.01% phosphoric acid) in a ratio 45/55 (v v<sup>-1</sup>), injection volume of 30 µL, flow rate of 1.0 mL min<sup>-1</sup>, wavelength of 254 nm and column oven temperature of 30 °C. The mobile phase showed good linearity in a range of 0.1 to 8 mg L<sup>-1</sup> of metribuzin. The analytical curve showed a coefficient of determination (R<sup>2</sup>) equal to 0.9993. The limit of detection (LoD) and quantification (LoQ) were 0.044 and 0.13 mg L<sup>-1</sup>, respectively.

In the desorption study, the sorption supernatant was discarded from the Falcon tubes containing biochar-amended and unamended soils and then 10 mL of the new 0.01 mol L<sup>-1</sup> CaCl<sub>2</sub> solution without herbicide was added. The tubes were subjected to rotary shaking for 24 h until they reached the re-equilibrium concentration. Subsequently, the tubes were centrifuged at 3500 rpm for 7 min. A 2 mL aliquot was filtered and placed in a vial for HPLC analysis. The amount desorbed was calculated as the difference between the sorbed metribuzin in the soil and the amount remaining in the supernatant.

#### 2.4. Freundlich Model for Sorption–Desorption and Apparent Coefficient

The sorption apparent coefficient ( $K_{d-app}$ , L kg<sup>-1</sup>) was also calculated at  $C_e = 2.0$  mg L<sup>-1</sup> (an intermediate value of the equilibrium concentrations studied in the sorption), using the following Equation (1):

$$K_{d-app} = C_s / C_e \quad (1)$$

where  $C_s$  is the amount of herbicide sorbed in the unamended and biochar-amended soil (mg kg<sup>-1</sup>) (2):

$$C_s = (C_i - C_e) \times V / M \quad (2)$$

where  $C_i$  is the pesticide initial liquid concentration (mg L<sup>-1</sup>),  $C_e$  is the equilibrium liquid concentration (mg L<sup>-1</sup>),  $V$  is the volume of herbicide solution added (mL) and  $M$  is the mass of soil (g) [13].

The sorption coefficient ( $K_{d-app}$ , L kg<sup>-1</sup>) normalized to the OC content of the biochar-amended and unamended soils ( $K_{oc}$ , L kg<sup>-1</sup>) was calculated as follows (3):

$$K_{oc} = (K_{d-app} / \%OC) \times 100 \quad (3)$$

The desorption  $K_{d-app}$  value for desorption was also calculated for comparison to the sorption  $K_{d-app}$ .

The Freundlich model and its distribution coefficient were derived from Equation (4):

$$K_f = C_s / C_e^{1/n} \quad (4)$$

where  $n$  (dimensionless value) can range from 0 to 1, depending on the heterogeneity in the sorption sites.

The same sorption coefficient was also standardized, considering the soil OC content ( $K_{foc}$ ). The hysteresis index (H) was calculated by Equation (5):

$$H = 1/n_{sorption} / 1/n_{desorption} \quad (5)$$

The thermodynamic parameter of Gibbs free energy ( $\Delta G$ ) to evaluate the degree of spontaneity of the sorption process was calculated by linear equation of van't Hoff (6). The average  $K_f$  (Freundlich coefficient) value of each treatment was used for the calculation.

$$\Delta G = - R \cdot T \cdot \ln K_f \quad (6)$$

where  $R$  is the gas constant (8314 J mol<sup>-1</sup> K<sup>-1</sup>),  $T$  is the absolute temperature (298 K) and  $K_f$  is the Freundlich coefficient (mg<sup>(1-1/n)</sup> L<sup>1/n</sup> kg<sup>-1</sup>).

### 3. Results and Discussion

#### 3.1. Biochar Characterization

All biochar attributes varied as the pyrolysis temperature of the production system increased. The pH of BC350 was lower (8.6) than BC550 (9.3) and BC750 (9.8). BC750 increased the SSA 13-fold compared to BC350. Higher C/N ratio and ash content were observed for BC750 (Table 1). These results are in agreement with what has been observed in studies with different pyrolysis temperatures in sugarcane straw biochar [32,38,39]. The increase in pyrolysis temperature influences the SSA of biochar because there is a change in the carbon structure, with the formation of structures similar to graphene, which has a larger pore volume and, consequently, SSA [11]. The higher pH values of the biochar produced at high temperature (BC750) are positively correlated with carbonate formation, inorganic alkali content and increased ash content [40,41]. Ashes are mainly responsible for the generation of alkalinity in biochar, due to the presence of alkaline-reacting minerals, such as  $\text{Na}^+$ ,  $\text{Ca}^{2+}$  and  $\text{Mg}^{2+}$  [42]. The higher SSA of BC750 is probably related to the release of volatile substances present in the biomass and the change in the C structure, increasing the SSA and pore volume through degradation of OM [43,44]. The higher C/N ratio of BC750 may be related to N losses during the thermal production process. With increasing pyrolysis temperature, usually compounds with higher C content and lower N content are formed, because N is lost through volatilization at high temperatures [45]. Increases in C/N ratios may indicate the production of compounds that have higher levels of recalcitrant C [46].

The elemental composition of biochar is shown in Supplementary Material (Figure S1B), represented by the atomic percentage of elements located in EDS images (Figure S1A). C was predominant for the biochar produced at the three pyrolysis temperatures (BC350, BC550 and BC750) with values of ~90%. The O was 4.48, 8.04 and 12.6% for the BC350, BC550 and BC750, respectively. Higher percentages of the elements Mg, Ca, Al, P, K and Si were observed for BC550 and BC750. The increase in inorganic constituents in pyrolyzed biochar at high temperatures is related to the higher ash content that remains in the biochar after carbonization [47]. The characteristics of the biochar surface are presented in Figure S2. BC350 preserved the structural organization of the plant cell wall with a lamellar structure on the surface [48]. High pyrolysis temperatures showed deformation of the biochar surface, which was also observed by [49] when comparing biochars derived from wheat, corn, rape and rice straw at different pyrolysis temperatures.

The increase in pyrolysis temperature promoted a reduction in the amount of organic functional groups in the biochar (Figure 1A). The results of the FTIR spectrum showed variation in peaks and absorption intensity with variation in pyrolysis temperature. For BC350, a band is observed at  $788\text{ cm}^{-1}$  that can be attributed to aromatic and alkali functional groups, such as C=C [50], a band at  $1040\text{ cm}^{-1}$  that can be assigned to the C-O vibration [51], a band at  $1580\text{ cm}^{-1}$  that can be attributed to aromatic groups elongating the C=C bond [52], a band at  $2095\text{ cm}^{-1}$ , which is assigned to asymmetric aliphatic C-H stretches [53] and a band at  $2100\text{ cm}^{-1}$ , assigned to C=C stretching [54]. The increase in pyrolysis temperature directly influenced the surface functional groups and may be attributed to the structural reorganization of biochar through depolymerization and volatilization due to ion losses of carbonaceous compounds ( $\text{H}^+$  and  $\text{O}^-$ ) [55,56]. The decrease in intensity of the aliphatic elongation (C-H) bands was also observed by [32] and is attributed to dehydration of the lignin and/or cellulose compounds, as well as structural changes in the aliphatic compounds.

The Raman spectra of all materials (Figure 1B) showed classical bands of carbonaceous materials, i.e., D and G located in the first-order region,  $1100$  to  $1800\text{ cm}^{-1}$ . In the spectra, it was possible to observe that BC350 showed higher intensity for the G band compared to the D band when compared to BC550 and BC750. The analysis of the organizational structure of the biochars, analyzed by Raman spectrum, indicated that material synthesized at the minimum temperature (BC350) has a more organized structure and, although all biochars have well-defined D and G bands, their intensities are close. This indicates that

these materials have some degree of structural defects [57]. Raman spectra of samples of different biochars show a D-band at 1337–1361  $\text{cm}^{-1}$  due to the A<sub>1g</sub> symmetry breathing mode that is non-existent in perfect graphite and, thus, only becomes active in the presence of disturbances, often referred to as amorphous C [51]. The G band (1596–1604  $\text{cm}^{-1}$ ) is related to the presence of carbon with sp<sup>2</sup> hybridization, more specifically, the vibration of the double bonds (C=C) that form the graphitic planes of the materials [58]. The higher the value of the ratio between the intensities of the D and G bands ( $I_D/I_G$ ), the lower the organization of the structure [59].

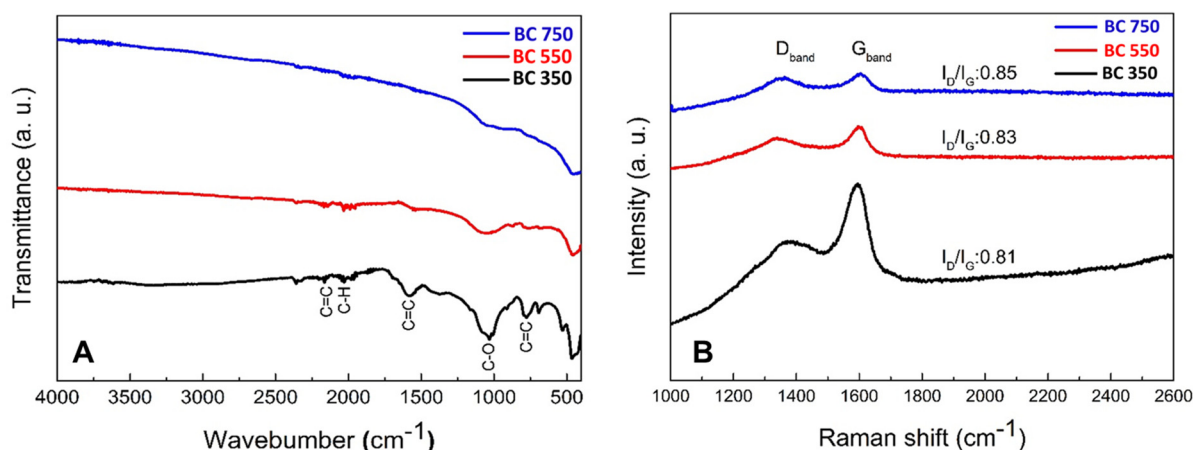


**Figure 1.** Fourier-transform infrared spectroscopy (FTIR) (A) and Raman spectra (B) of sugarcane straw biochar (BC) produced at pyrolysis temperatures of 350, 550 and 750 °C.

The physicochemical characteristics of biochar directly influence its sorptive capacity due to the distinct mechanisms of interaction between the herbicide molecule and the biochar. The nature of these interactions can be exclusively physical, chemical or both and result in the phenomenon of sorption [60]. The characteristics that directly influence the sorption of herbicides are related to porosity, SSA, aromatic structures, C contents, surface functional groups, pH and elemental composition [61]. Understanding the probable mechanisms for herbicide sorption by biochar ensures an understanding of the ability of each material to act as a potential soil remediator.

### 3.2. Characterization of Biochar-Amended and Unamended Soils

The chemical characteristics of the soils amended with BC350, BC550 and BC750 at different application rates are shown in Table 2. The pH of the amended soil with application rates 1.5%, regardless of pyrolysis temperature, increased the pH by ~0.5 units relative to the unamended soil. Higher pH values were observed for the soil amended with BC750, where the application rates of 5 and 10% increased pH by 1.7 and 2.1 units, respectively, relative to the unamended soil. The potential acidity (H + Al) in the biochar-amended soil, regardless of pyrolysis temperature, was similar to the unamended soil ( $33 \text{ mmol}_c \text{ kg}^{-1}$ ) for application rates < 1.0% (Table 2). Amended soil with 10% of BC350, BC550 and BC750 reduced potential acidity by 80, 90 and 100%, respectively. The increase in pH and reduction in potential acidity of the amended soil is possibly related to the amount of ash and basic cations in the biochar. Biochar can have a soil liming capacity due to the presence of basic cations (Ca, K, Mg and Si) that can form alkaline oxides or carbonates during the pyrolysis process and, once added to the soil, react with monomeric H + Al, increasing soil pH and, consequently, reducing exchangeable acidity [62]. One study, analyzing a 3% application rate of rice straw biochar to a soil with a pH of 5.24, reported increased soil pH by 4.5 units compared to the control [63].

The OC content of the unamended soil was 1.2% and increased to 1.3 and 1.4 in the amended soils, with application rates of 5 and 10% of BC750, respectively. The 10% application rate of BC550 increased the OC content to 1.3%. Regardless of the application

rate, no changes in OC were observed for the soil amended with BC350 (Table 2). The OC was also analyzed in a soil amended with six biochars [64]. These authors observed that OC content increased from 4.9% of the unamended soil to 5.4 and 5.2% in the amended soil with peanut shell and cassava bagasse biochar, respectively, and it was attributed to the higher OC content in the feedstocks, which is indicative that biochar applications to soils can increase C accumulation and sequestration.

Amended soil with BC350, BC550 and BC750 increased P for all application rates (Table 2). The rates application < 1.0% of biochar, regardless of pyrolysis temperature, increased the P concentration ~2-fold relative to unamended soil. The soil amended with 10% of BC350, BC550 and BC750 increased P by ~23-, 25- and 5-fold, respectively, relative to the unamended soil. Increases in P availability in amended soil with different biochars have been reported by different authors [65–67]. This result is directly related to the increase in pH and the change in the sorption site of P by the biochar-amended soil. P in more acidic soils is prone to complexing with Al or Fe and increasing soil pH above 7 may result in precipitation of free Al and Fe and, thus, decrease active P sorption sites [68]. The increased availability of P to the soil amended with BC750 is possibly related to characteristics of the biochar produced at high temperature, such as surface area and changes in soil exchange sites, preventing the fixation of P [69]. A study analyzed the potential of corn stover biochar produced at a pyrolysis temperature of 500 °C on the availability of P in soil [8]. The authors observed that P increased by 2.6-fold for 2% application rate, relative to the control soil.

K content in the amended soils increased for all application rates (Table 2). The 0.1% application rate of biochar, independent of pyrolysis temperature, increased the K in the amended soil by ~1.3-fold compared to the unamended soil. The 10% application rate of BC350, BC550 and BC750 increased the K by 3.7-, 4.4- and 7-fold, respectively, over unamended soil. Biochar typically contains a large proportion of K, which is dependent on pyrolysis temperature and feedstock [70]. For mild pyrolysis temperatures < 500 °C, the C and N contents are volatile; however, K starts to volatilize at higher temperatures > 700 °C, which provides an increase in K concentration in the biochar produced at high temperature [71]. Amended soil with 0.3% application rate of cassava stem biochar and rice husk were analyzed for K [72]. The authors reported release of ~148 mg kg<sup>-1</sup> of K after 7 d of incubation of amended soil with cassava stem biochar and ~188 mg kg<sup>-1</sup> of K after 1 d of incubation for rice husk biochar, being two biochars with high potential for K accumulation in soil.

Ca and Mg contents increased with soil modification with biochar; however, small variations were observed between application rates and pyrolysis temperature (Table 2). Application rate of 10% biochar, regardless of pyrolysis temperature, increased Ca and Mg by ~1.2- and 1.9-fold, respectively, relative to unamended soil. The increase in Ca was also observed in a study with six different biochars [64]. The authors observed that compared to the unamended soil, the Ca content increased by 1.2–5.9%.

The contents of the micronutrients Zn, Cu and B showed no variations in relation to the unamended soil, for all pyrolysis temperatures and application rates (Table 2). Fe and Mn contents increased ~2-fold, relative to unamended soil, for the 10% application rate, regardless of pyrolysis temperature (Table 2). In more alkaline soils (pH > 7.0), Zn and Cu can form associations with Fe oxides and their availability in the soil solution is decreased. The application of different rates of hardwood biochar (*Quercus* spp. and *Carya* spp.) to alkaline soils was analyzed in terms of soil chemical modifications [73]. The authors observed that increasing the application rate of biochar provided higher Fe and Mn content but showed no effect for Zn and Cu in the amended soil.

The CEC was similar to unamended soil (23.3 mmol<sub>c</sub> kg<sup>-1</sup>) for application rates < 1.0%, regardless of pyrolysis temperature. Amended soil with 10% of BC350, BC550 and BC750 increased CEC by 1.6-, 1.65- and 1.7-fold, respectively, compared to unamended soil. The mechanisms that increase the SSA of the amended soil are probably mediated by the higher SSA, negative surface charge and charge density in the biochar [74], and the increase in soil pH, as presented in this study. Increased pH after biochar addition may

result in deprotonation of functional groups of minerals, such as kaolinite, resulting in the development of negative charges that increase the CEC of the amended soil [75].

The BS of the soil amended with BC350, BC550 and BC750 increased to 85, 90 and 100% at 10% application rate. Similar results were observed in the application of poultry litter biochar produced at 350 °C [76]. The authors reported increased soil BS of 33.58% and 43.28% for the two highest application rates (0.4 and 0.5%, respectively) when compared to unamended soil.

Overall, the sugarcane straw biochar produced at different pyrolysis temperatures directly influenced soil fertility when applied at high rates (5 and 10%). However, application rates of 1 and 1.5% have potential in reducing potential acidity, increasing pH, high P and K contents, maintaining Ca and Mg values and the micronutrients Fe and Mn and improving soil CEC. Improvements in soil chemical attributes are provided by adding application rates of 1 to 1.5% of BC350, BC550 and BC750 of sugarcane straw and may be an alternative for soil fertility.

### 3.3. Sorption–Desorption Metribuzin in Biochar-Amended and Unamended Soils

The sorption–desorption isotherms were adequately fitted using the Freundlich model to describe the sorption–desorption of metribuzin in amended soil at different biochar application rates and pyrolysis temperature, as indicated by the high coefficients of determination ( $R^2 \geq 0.98$ ) of the equations (Figures 2 and 3). The degree of linearity ( $1/n$ ) ranged from 0.34 to 0.89 for sorption and 0.41 to 1.05 for desorption, indicating that the sorption and desorption isotherm is classified as type L (Tables 3 and 4). This type of isotherm is indicative that the sorbent (biochar-amended soil) showed lower sorption capacity at high concentrations of the sorbate (herbicide) [77]. Thus, at low concentrations, metribuzin showed higher affinity for biochar-amended soil, due to the high availability of sorption sites at higher application rates (>1.5%), independent of pyrolysis temperature. As the concentration of metribuzin increased, the number of binding sites decreased and the concentration in the soil solution increased, consequently reducing its sorption by the biochar-amended soil. This behavior was also observed for the sorption of metribuzin on biochar from grapevine pruning residues and bonechar (cow bone) [26,27].

According to the sorption coefficients (Table 3), for both the Freundlich model ( $K_f$ ) and the median concentration ( $K_{d-app}$ ), metribuzin showed increasing sorption as the biochar application rate to the soil increased. The  $K_f$  value was low for unamended soil ( $1.42 \text{ mg}^{(1-1/n)} \text{ L}^{1/n} \text{ kg}^{-1}$ ). Studies analyzing the sorption and desorption of metribuzin in different soils have reported sorption  $K_f$  values between 0.18 and  $2.5 \text{ mg}^{(1-1/n)} \text{ L}^{1/n} \text{ kg}^{-1}$ , being dependent on clay content, OM and soil pH [27,78–80].

BC750-amended soil improved the sorption of metribuzin between 1 and 10-fold over unamended soil as application rates increased from 0.1 to 10%. BC350- and BC550-amended soils showed similar sorption with ~1.3- and 6-fold increases in sorption at application rates of 1.5 and 10%, respectively, compared to unamended soil. The  $K_f$  and  $K_{d-app}$  of the sorption of metribuzin were normalized by the OC content in the soil, showing that the overall sorption trends were not altered by the OC (Table 3). The  $K_{foc}$  values for the sorption of metribuzin on the amended soil increased proportionally to the application rate and pyrolysis temperature. The  $K_{foc}$  for the 10% application rate was 504, 726 and  $1236 \text{ mg}^{(1-1/n)} \text{ L}^{1/n} \text{ kg}^{-1}$  for the amended soil with BC350, BC550 and BC750, respectively (Table 3). The higher sorption of metribuzin in the soil amended with BC750 can be attributed to the higher SSA compared to BC350 and BC550. The increased sorption capacity of biochar is directly related to higher SSA, because the number of pores increases proportionally with SSA, providing a greater number of herbicide binding sites [81]. The  $K_f$  value of metribuzin sorption was evaluated in a study with sugarcane bagasse biochar, produced at different pyrolysis temperatures [82]. These authors observed that the biochar produced at 700 °C presented  $K_f$  of  $47.2 \text{ mg}^{(1-1/n)} \text{ L}^{1/n} \text{ kg}^{-1}$  and SSA of  $82 \text{ m}^2 \text{ g}^{-1}$ , while for the biochar produced at 350 °C, the  $K_f$  was  $9.77 \text{ mg}^{(1-1/n)} \text{ L}^{1/n} \text{ kg}^{-1}$  and SSA was  $2.6 \text{ m}^2 \text{ g}^{-1}$ .

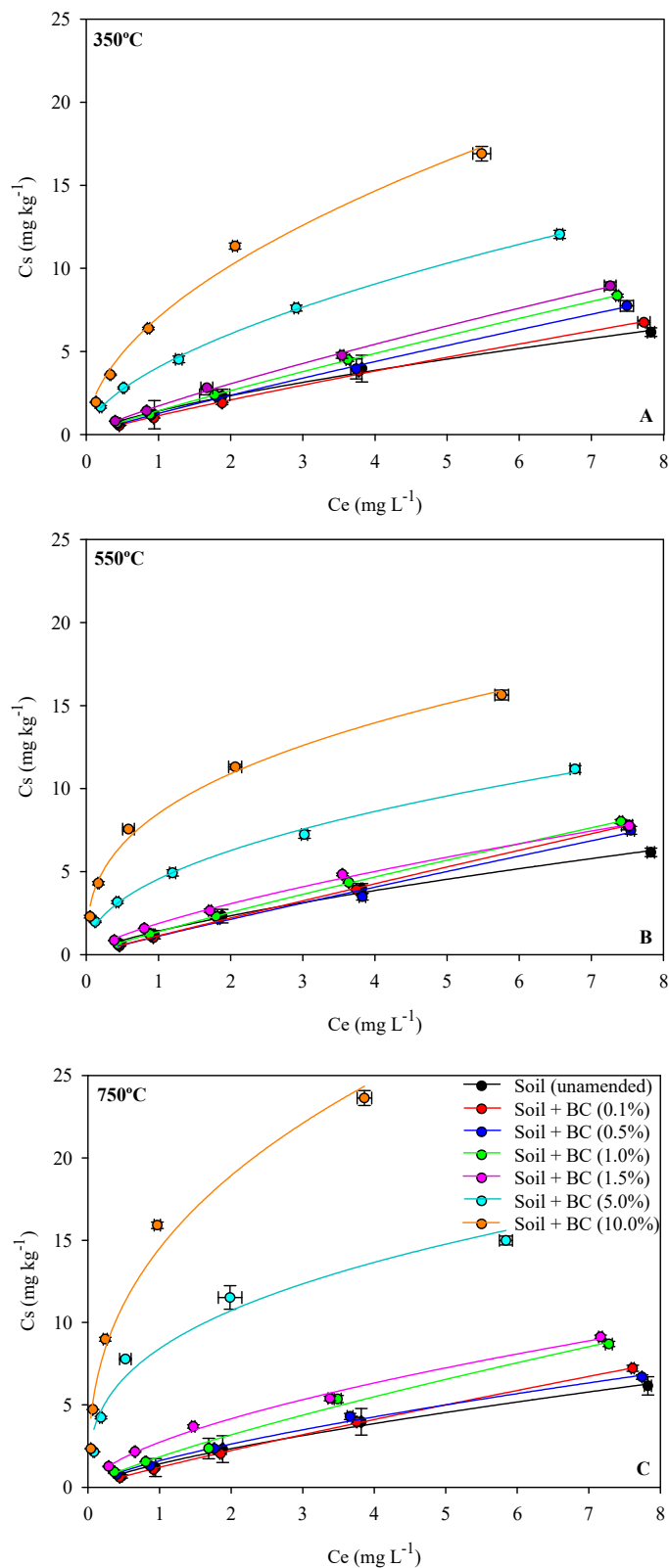


**Figure 2.** Sorption isotherms of the Freundlich model of metribuzin applied in soil amended and unamended (control) with sugarcane straw biochar (BC) produced at pyrolysis temperatures of 350 °C (A), 550 °C (B) and 750 °C (C). The vertical and horizontal bars represent standard error ( $n = 3$ ) of  $C_e$  (equilibrium concentration) and  $C_s$  (soil concentration). Symbols can cover the bars.

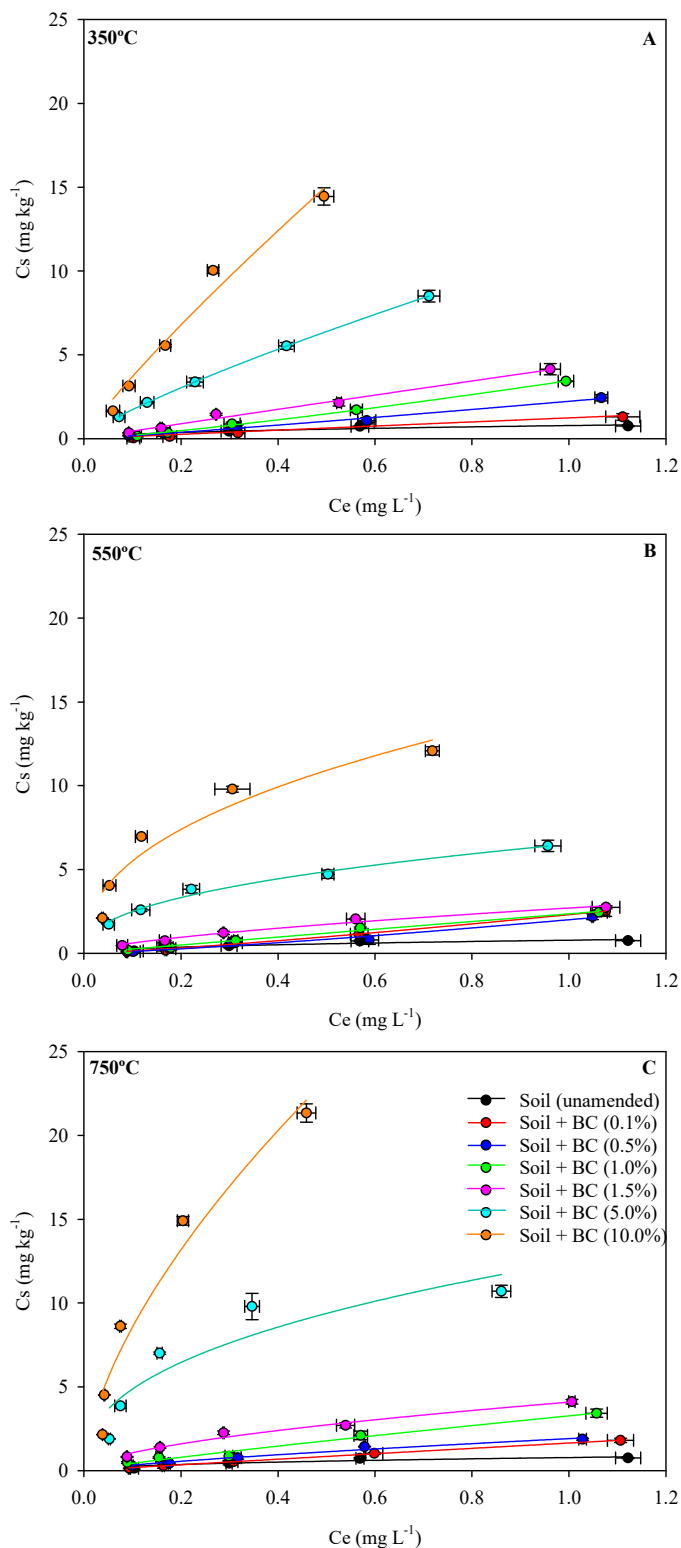


**Figure 3.** Desorption isotherms of the Freundlich model of metribuzin applied in soil amended and unamended (control) with sugarcane straw biochar (BC) produced at pyrolysis temperatures of 350 °C (A), 550 °C (B) and 750 °C (C). The vertical and horizontal bars represent standard error ( $n = 3$ ) of  $C_e$  (equilibrium concentration) and  $C_s$  (soil concentration). Symbols can cover the bars.

**Table 3.** Sorption isotherm parameters of Freundlich model. Sorption coefficient ( $K_{d-app}$ ) of 2 mg L<sup>-1</sup> and Gibbs free energy ( $\Delta G$ ) concentration for metribuzin applied to soil amended with sugarcane straw biochar and unamended soil.

Pyrolysis Temperature (°C)	Application Rate (%) w w <sup>-1</sup>	Freundlich					$K_{d-app}$ L kg <sup>-1</sup>	$K_{oc}$ Sorbed (%)	$\Delta G$ kJ mol <sup>-1</sup>
		$K_f$ (mg <sup>(1-1/n)</sup> L <sup>1/n</sup> kg <sup>-1</sup> )	$K_{foc}$	$1/n$	$R^2$				
-	unamended	1.42 ± 0.26 <sup>a</sup>	114.5	0.721 ± 0.04	0.99	1.66 ± 0.71	133	23.17 ± 2.80	-868.77
	0.1	1.13 ± 0.05	96	0.875 ± 0.05	0.99	0.96 ± 0.07	82	18.9 ± 0.28	-302.80
	0.5	1.27 ± 0.14	116	0.894 ± 0.03	0.99	1.39 ± 0.14	127	22.8 ± 0.76	-592.18
	1	1.33 ± 0.05	122	0.885 ± 0.03	0.99	1.37 ± 0.04	117	23.8 ± 0.48	-706.55
	1.5	1.71 ± 0.10	137	0.830 ± 0.01	0.99	1.60 ± 0.10	129	28.0 ± 0.61	-1329.20
	5	4.05 ± 0.15	311	0.579 ± 0.02	0.99	3.04 ± 0.34	233	45.2 ± 1.56	-3465.42
	10	7.06 ± 0.16	504	0.527 ± 0.01	0.99	6.99 ± 0.11	499	63.8 ± 0.98	-4842.27
350	0.1	1.21 ± 0.08	105	0.807 ± 0.02	0.99	1.22 ± 0.15	104	20.4 ± 0.62	-472.27
	0.5	1.38 ± 0.10	117	0.877 ± 0.03	0.99	1.23 ± 0.05	105	21.9 ± 0.72	-797.98
	1	1.13 ± 0.08	91	0.854 ± 0.01	0.99	1.33 ± 0.23	107	22.0 ± 0.82	-302.80
	1.5	1.87 ± 0.04	159	0.708 ± 0.02	0.99	1.58 ± 0.16	134	26.4 ± 0.39	-1550.80
	5	4.55 ± 0.15	417	0.460 ± 0.02	0.99	4.77 ± 0.32	437	49.2 ± 1.38	-3753.83
	10	8.50 ± 0.10	726	0.358 ± 0.02	0.99	14.0 ± 0.14	1196	75.5 ± 0.74	-5302.16
550	0.1	1.54 ± 0.07	107	0.881 ± 0.01	0.99	1.03 ± 0.09	83	23.6 ± 0.56	-532.95
	0.5	1.60 ± 0.09	136	0.704 ± 0.03	0.99	1.35 ± 0.18	115	23.4 ± 0.75	-1164.46
	1	1.84 ± 0.21	157	0.788 ± 0.06	0.99	1.09 ± 1.0	93	23.5 ± 1.90	-1510.73
	1.5	2.73 ± 0.08	220	0.606 ± 0.03	0.99	2.58 ± 0.17	208	39.9 ± 0.79	-2488.22
	5	8.41 ± 0.22	718	0.349 ± 0.04	0.98	14.2 ± 0.18	1210	77.8 ± 1.31	-5275.79
	10	14.51 ± 0.15	1239	0.383 ± 0.06	0.98	45.0 ± 0.21	3846	89.4 ± 0.70	-6627.10

<sup>a</sup> Average of the value of each parameter ± standard deviation of the mean (n = 3).

**Table 4.** Desorption isotherm parameters of Freundlich model. Sorption coefficient ( $K_{d-app}$ ) of 2 mg L<sup>-1</sup>. Hysteresis coefficient (H) and Gibbs free energy ( $\Delta G$ ) for metribuzin applied to soil amended with sugarcane straw biochar and unamended soil.

Pyrolysis Temperature (°C)	Biochar Application Rate (%) w w <sup>-1</sup>	Freundlich					$K_{d-app}$ L kg <sup>-1</sup>	$K_{oc}$	$\Delta G$ kJ mol <sup>-1</sup>	
		$K_f$ (mg <sup>(1-1/n)</sup> L <sup>1/n</sup> kg <sup>-1</sup> )	$K_{foc}$	$1/n$	H	$R^2$				
-	unamended	0.78 ± 0.09 <sup>a</sup>	62	0.468 ± 0.13	0.65	0.91	1.49 ± 0.09	117	15.8 ± 0.54	-615.58
	0.1	1.23 ± 0.08	105	0.974 ± 0.30	1.11	0.96	1.07 ± 0.04	91	15.5 ± 0.25	-512.89
	0.5	2.22 ± 0.18	203	1.006 ± 0.10	1.24	0.99	2.27 ± 0.10	208	15.7 ± 0.45	-1975.88
	1	3.45 ± 0.06	294	1.029 ± 0.04	1.39	0.99	2.86 ± 0.10	244	15.1 ± 0.72	-3068.16
	1.5	3.27 ± 0.12	344	0.976 ± 0.08	1.18	0.99	5.33 ± 0.06	429	13.5 ± 0.15	-2935.40
	5	6.51 ± 0.18	597	0.418 ± 0.03	0.91	0.99	14.76 ± 0.07	1135	11.0 ± 0.32	-5985.60
	10	14.64 ± 0.11	1251	0.425 ± 0.07	1.19	0.96	33.10 ± 0.07	2364	5.8 ± 0.19	-8218.33
350	0.1	2.30 ± 0.09	196	1.023 ± 0.06	1.52	0.99	2.03 ± 0.07	173	15.2 ± 0.13	-2062.59
	0.5	2.00 ± 0.08	170	1.059 ± 0.20	1.44	0.97	2.21 ± 0.03	188	15.1 ± 0.30	-1717.32
	1	2.35 ± 0.09	189	0.970 ± 0.08	1.02	0.99	2.40 ± 0.14	193	15.5 ± 0.23	-2116.87
	1.5	2.69 ± 0.05	229	0.645 ± 0.05	0.91	0.99	4.23 ± 0.10	361	14.3 ± 0.18	-2451.65
	5	11.28 ± 0.17	961	0.818 ± 0.03	0.91	0.99	17.26 ± 0.22	1583	11.4 ± 0.44	-4641.33
	10	27.58 ± 0.18	1970	0.815 ± 0.07	1.19	0.96	58.86 ± 0.09	5030	8.3 ± 0.32	-6649.20
550	0.1	1.64 ± 0.06	132	0.960 ± 0.02	1.09	0.99	1.72 ± 0.09	138	15.1 ± 0.37	-1225.61
	0.5	1.90 ± 0.18	162	0.766 ± 0.09	1.09	0.98	2.40 ± 0.07	205	15.7 ± 0.26	-1590.23
	1	3.26 ± 0.12	281	0.877 ± 0.09	1.11	0.99	7.02 ± 0.03	600	14.9 ± 0.33	-2927.80
	1.5	4.08 ± 0.09	329	0.583 ± 0.05	0.96	0.99	7.85 ± 0.11	566	14.3 ± 0.18	-3483.70
	5	12.44 ± 0.27	1063	0.468 ± 0.10	1.34	0.91	44.9 ± 0.06	3837	11.8 ± 0.31	-6245.75
	10	35.91 ± 0.19	3069	0.623 ± 0.09	1.62	0.97	114.5 ± 0.13	9786	3.7 ± 0.17	-8872.22

<sup>a</sup> Average of the value of each parameter ± standard deviation of the mean (n = 3).

FTIR analysis showed that with increasing pyrolysis temperature, losses of surface functional groups occurred, which may increase the sorptive capacity of BC750. Low-temperature biochar (350 °C) has more polar, aliphatic surface groups that are amorphous in character [83], while high-temperature biochar has surface groups that resemble graphitic aromatic C, rich in  $\pi$  electrons [84]. The increased sorption capacity on BC750 could also occur due to  $\pi$ - $\pi$ -type binding between metribuzin and BC750. Triazine herbicides, such as metribuzin, can behave as a  $\pi$ -electron donor while the polyaromatic surfaces of biochar act as an electron acceptor, indicating a combination of a  $\pi$ - $\pi$  force between metribuzin and the biochar surface [85]. Wheat straw biochar produced at a pyrolysis temperature of 800 °C

was analyzed for the sorption potential of metribuzin for environmental remediation [86]. These authors observed that the predominant sorption process was linked to chemical sorption via  $\pi$ - $\pi$  interactions.

The pH has an influence on the sorption and desorption of metribuzin in the amended soil. Metribuzin is a strong acid ( $pK_a = 1.3$ ) and shows low sorption due to its ionic form (negatively charged) that provides repulsion with the negative charges of the soil under conditions of high pH values [78,87]. However, even as the pH of the biochar-amended soil increased, the sorption of metribuzin was higher than in the unamended soil. Although the herbicide is mostly in ionic form, the mechanisms related to porous structure, SSA and surface groups provide high capacity to sorb the herbicides that are in the soil solution [88]. Similar results were observed by [89], analyzing pH and biochar addition on the sorption of two acidic herbicides (2,4-D and imazethapyr). The authors observed that in unamended soil, sorption decreased as soil pH increased, providing injury to the rice crop. As 2 and 8% biochar were added to the soil, pH increased; however, sorption increased proportionally, decreasing crop injury.

The application rates of biochar produced at different pyrolysis temperatures influenced the percentage sorbed (relative to the total initially applied) of metribuzin in the soil (Table 3). Application rates of 0.1, 0.5 and 1% biochar had similar percentages of metribuzin sorbed to unamended soil (~23%) for all pyrolysis temperatures. The 5% application rate of BC750 to soil increased the sorption of metribuzin by 70%, while amended soil with BC350 and BC550 sorbed 45 and 49%, respectively. At the highest application rate, the percentage of metribuzin sorbed was 63.8, 75.5 and 89.4% relative to the total applied, for the amended soil with BC350, BC550 and BC750, respectively (Table 3). The presence of 5% biochar can directly influence the effectiveness of metribuzin in the soil for weed control. Sugarcane straw biochar with a high sorptive capacity, such as BC750, applied at high rates may result in a scenario where even higher doses will be required to control weeds after the addition of this material to the area. However, the application of biochar to soil for agronomic purposes is considered undesirable [61]. In a remediation scenario for soils contaminated with metribuzin, sugarcane straw biochar presented itself as a viable alternative for immobilization of the herbicide at application rates above 5%.

Increased sorption of metribuzin at higher application rates was observed using different biochars [25,90,91]. Application rates of olive mill waste biochar were analyzed for the sorption potential of metribuzin in the soil [25]. These authors observed that the application of 2.5 and 5% biochar increased the sorption of metribuzin by 1.5- and 2.5-fold, respectively, relative to unamended soil. The effectiveness of metribuzin was reduced when sugarcane bagasse biochar was applied (350 and 700 °C) at rates of 1 to 4% in clayey soil [82]. The authors observed that the application rate of 8% biochar reduced the residual effect of metribuzin and provided increased germination of Palmer amaranth (*Amaranthus palmeri*), being larger than the unamended soil. The reduction in herbicide residual effect was also observed by [92], in which an application rate of only 1.6% of bonechar in the soil was sufficient to reduce the level of weed injury by 50%.

The desorption coefficients (Table 4) for the Freundlich model ( $K_f$ ) and at the median concentration ( $K_{d-app}$ ) showed that desorption was reduced as the application rate of biochar to the soil increased. The  $K_f$  value of the unamended soil desorption was  $0.78 \text{ mg}^{(1-1/n)} \text{ L}^{1/n} \text{ kg}^{-1}$ . The desorption of metribuzin decreased between 2- and 46-times for the application rate of 0.1 to 10% for the BC750-amended soil compared to the unamended soil. Soil amended with BC350 and BC550 decreased desorption by up to 18- and 35-fold, respectively, for the 10% application rate, relative to unamended soil. The higher  $K_f$  (desorption) value for metribuzin in the amended soils, relative to the unamended soil, regardless of pyrolysis temperature, indicated that the presence of carbonaceous material decreased the desorption of metribuzin. Lipophilic herbicides, such as metribuzin ( $\text{Log } K_{ow} = 1.75$ ), can establish chemical interactions between non-polar groups in the biochar and increase stability, reducing desorption. Both the C content and the aromatic

structure are important factors affecting the low desorption capacity of biochar for lipophilic herbicides [13,93].

The percent of metribuzin desorbed in the soil with application rates of 0.1, 0.5 and 1% biochar was similar to the unamended soil (~15%) at all pyrolysis temperatures (Table 4). The 10% application rate of biochar to soil provided the least desorption of metribuzin, being desorbed 8.3, 5.8 and 3.7% for BC350, BC550 and BC750, respectively. The desorption  $K_{foc}$  values for the 10% application rate were 1970, 1251 and 3069  $\text{mg}^{(1-1/n)} \text{L}^{1/n} \text{kg}^{-1}$  in the BC350-, BC550- and BC750-amended soils, respectively. The hysteresis (H) of the isotherms of metribuzin in the unamended soil was 0.65 and when biochar was added, the H was greater than 1, which is classified as negative hysteresis ( $H > 1$ ) (Table 4). When H is negative, it indicates that desorption is greater than the sorption rate [94]. With increasing application rates of BC750 biochar, the H values increased, showing that the application of this biochar can decrease the bioavailability of metribuzin in the soil solution. Metribuzin also showed negative H in soils amended with fly ashes [95]. The results of the lower desorption of metribuzin presented in this study showed that, in addition to the high sorption capacity, the sugarcane straw biochar presented available pores for herbicide diffusion. The porous structures of biochar can lead to herbicide immobilization [96]. The lowest desorption of atrazine was also observed when applied directly to the amended soil with biochar from cassava waste obtained at 750 °C [97]. The authors reported that the lower desorption could be related to the irreversibility of chemical bonding or sequestration of atrazine in meso- or micro-pores of the biochar.

In general, the Gibbs free energy value ( $\Delta G$ ) of the sorption and desorption reaction of metribuzin in the biochar-amended soils decreased with increasing pyrolysis temperature and application rates (Tables 3 and 4). This indicates that as pyrolysis temperature and application rates increased, the molecules of this herbicide remained sorbed onto the biochar, indicating that sorption increased while desorption decreased. The change in Gibbs free energy ( $\Delta G$ ) indicates the degree of spontaneity in a sorption process and a larger negative value reflects more energetically favorable sorption [98]. The more negative  $\Delta G$  value for the BC750-amended soil (Table 3) indicated that sorption of metribuzin was not exclusively governed by chemical reactions, since an absolute  $\Delta G$  value of less than 40 kJ/mol indicates mainly physical sorption [99]. However, both physical and chemical sorption are processes that can occur concomitantly [100]. Sorption is a thermodynamic process, i.e., physical sorption (related to surface interaction, pore filling, Coulomb forces, van der Waals and hydrogen bonds) and chemical sorption (valence forces, electron donor-acceptor (EDA) mechanisms,  $\pi$ -interactions) involve the conversion of heat and other forms of energy [60].

Overall, soil modification with higher application rates (1.5, 5 and 10%) of BC750 had a high influence on the sorption and desorption of metribuzin from the soil and may reduce the potential of the herbicide to control weeds. However, lower rates (<1.5%) of BC350 and 550 provided less impact on sorption and desorption of metribuzin and improved the chemical attributes in the amended soils. This information is important for determining the application of these biochars to the soil, either as fertilizer or to reduce the risk of environmental contamination of the herbicide. The sorption and desorption study showed that the successful use of biochar will depend on the relationship between pyrolysis temperature and application rate.

#### 4. Conclusions

Pyrolysis temperature altered the physicochemical attributes of sugarcane straw biochar. BC750C showed higher SSA, C/N ratio, pH and decreased presence of surface functional groups, which may be directly linked to higher sorption and lower desorption of metribuzin in the amended soil. The physicochemical characterization allows the analysis of the biochar composition and the main positive aspects related to herbicide immobilization.

Using application rates of 1 and 1.5% of BC350, BC550 and BC750 can improve soil fertility by making P, K, Mg, Fe and Mn available, reducing potential acidity (H + Al) and increasing soil pH. The lower rates of BC350 and 550 provided less impact on the sorption and desorption of metribuzin and may be an alternative for the use of sugarcane straw biochar produced at low pyrolysis temperatures as a source of fertilizer. However, it is important to note that the sorption and desorption behavior takes into account the physicochemical attributes of the herbicide; in this case, the same biochar evaluated in this study may present lower or higher sorption capacity when analyzed with another herbicide.

Soil amended with BC750, from an environmental remediation perspective, has a high potential to decrease the mobility and risks of metribuzin in environmental contamination. However, sorption of metribuzin increased and desorption decreased with increasing rates of biochar application, which may negatively affect the bioavailability of metribuzin in the soil solution and, in an agronomic approach, may influence the residual effect of metribuzin in the soil and decrease its activity in weed control efficacy.

**Supplementary Materials:** The following supporting information can be downloaded at: <https://www.mdpi.com/article/10.3390/pr10101924/s1>, Figure S1. Surficial elemental composition C (red), O (yellow), Si (green), Ca, K, P, Al, P and Na (undetected) by energy dispersive X-ray spectrometry (EDS) analysis of biochar (BC) (A) and EDS spectrogram (B) in different pyrolysis temperatures (350, 550 and 750 °C); Figure S2. Images of the biochar (BC) derived from sugar cane straw at different pyrolysis temperatures (350, 550 and 750 °C) by scanning electron microscopy (SEM) at 500- and 3000-times magnification.

**Author Contributions:** Conceptualization, K.C.M.; Data curation, K.C.M., A.F.S.L., M.G.d.S.B. and B.A.d.P.M.; Investigation, Methodology, Validation, A.F.S.L., T.G., K.C.M. and K.F.M.; Writing—review and editing, K.C.M. and K.F.M.; Project administration, Formal analysis, Funding acquisition, K.F.M. All authors have read and agreed to the published version of the manuscript.

**Funding:** This research was funded by Coordination for the Improvement of Higher Education Personnel (CAPES-88887.479265/2020-00), Foundation for Research Support of the State of Minas Gerais (FAPEMIG-2070.01.0004768/2021-84).

**Data Availability Statement:** Not applicable.

**Acknowledgments:** The authors thanks the Federal University of Viçosa and the Matheus Bortolanza Soares from the “Luiz de Queiroz” College of Agriculture, University of São Paulo for kindly donating the biochar.

**Conflicts of Interest:** The authors declare no conflict of interest.

## References

1. Lehmann, J.; Joseph, S. *Biochar for environmental management: An introduction*, In *Biochar for Environmental Management: Science, Technology and Implementation*; Lehmann, J., Joseph, S., Eds.; Routledge: New York, NY, USA, 2015; pp. 1–13.
2. Gul, S.; Whalen, J.K.; Thomas, B.W.; Sachdeva, V.; Deng, H. Physico-chemical properties and microbial responses in biochar-amended soils: Mechanisms and future directions. *Agric. Ecosyst. Environ.* **2015**, *206*, 46–59. [[CrossRef](#)]
3. Zhang, Y.; Wang, J.; Feng, Y. The effects of biochar addition on soil physicochemical properties: A review. *Catena* **2021**, *202*, 105284. [[CrossRef](#)]
4. Liang, B.; Lehmann, J.; Solomon, D.; Kinyangi, J.; Grossman, J.; O'Neill, B.; Skjemstad, J.O.; Thies, J.; Luizão, F.J.; Petersen, J.; et al. Black carbon increases cation exchange capacity in soils. *Soil Sci. Soc. Am. J.* **2006**, *70*, 1719–1730. [[CrossRef](#)]
5. Mosley, L.M.; Willson, P.; Hamilton, B.; Butler, G.; Seaman, R. The capacity of biochar made from common reeds to neutralise pH and remove dissolved metals in acid drainage. *Environ. Sci. Pollut. Res.* **2015**, *22*, 15113–15122. [[CrossRef](#)] [[PubMed](#)]
6. Woolf, D.; Amonette, J.E.; Street-Perrott, F.A.; Lehmann, J.; Joseph, S. Sustainable biochar to mitigate global climate change. *Nat. Commun.* **2010**, *1*, 1–9. [[CrossRef](#)]
7. Khadem, A.; Raiesi, F.; Besharati, H.; Khalaj, M.A. The effects of biochar on soil nutrients status, microbial activity and carbon sequestration potential in two calcareous soils. *Biochar* **2021**, *3*, 105–116. [[CrossRef](#)]
8. Karimi, A.; Moezzi, A.; Chorom, M.; Enayatizamir, N. Application of biochar changed the status of nutrients and biological activity in a calcareous soil. *J. Soil Sci. Plant Nutr.* **2020**, *20*, 450–459. [[CrossRef](#)]
9. Hussain, M.; Farooq, M.; Nawaz, A.; Al-Sadi, A.M.; Solaiman, Z.M.; Alghamdi, S.S.; Ammara, U.; Ok, Y.S.; Siddique, K.H. Biochar for crop production: Potential benefits and risks. *J. Soils Sediments* **2017**, *17*, 685–716. [[CrossRef](#)]

10. Bartoli, M.; Giorcelli, M.; Jagdale, P.; Rovere, M.; Tagliaferro, A. A review of non-soil biochar applications. *Materials* **2020**, *13*, 261. [CrossRef]
11. Ahmad, M.; Rajapaksha, A.U.; Lim, J.E.; Zhang, M.; Bolan, N.; Mohan, D.; Vithanagef, M.; Lee, S.S.; Ok, Y.S. Biochar as a sorbent for contaminant management in soil and water: A review. *Chemosphere* **2014**, *99*, 19–33. [CrossRef]
12. Yu, X.Y.; Mu, C.L.; Gu, C.; Liu, C.; Liu, X.J. Impact of woodchip biochar amendment on the sorption and dissipation of pesticide acetamiprid in agricultural soils. *Chemosphere* **2011**, *85*, 1284–1289. [CrossRef] [PubMed]
13. Cabrera, A.; Cox, L.; Spokas, K.U.R.T.; Hermosín, M.C.; Cornejo, J.; Koskinen, W.C. Influence of biochar amendments on the sorption-desorption of aminocyclopyrachlor, bentazone and pyraclostrobin pesticides to an agricultural soil. *Sci. Total Environ.* **2014**, *470*, 438–443. [CrossRef] [PubMed]
14. Huang, H.; Zhang, C.; Zhang, P.; Cao, M.; Xu, G.; Wu, H.; Zhang, J.; Li, C.; Rong, Q. Effects of biochar amendment on the sorption and degradation of atrazine in different soils. *Soil Sediment Contam.* **2018**, *27*, 643–657. [CrossRef]
15. Szmigielski, A.M.; Hants, R.D.; Schoenau, J.J. Bioavailability of metsulfuron and sulfentrazone herbicides in soil as affected by amendment with two contrasting willow biochars. *Bull. Environ. Contam. Toxicol.* **2018**, *100*, 298–302. [CrossRef]
16. Mendes, K.F.; Júnior, A.F.D.; Takeshita, V.; Régo, A.P.J.; Tornisielo, V.L. Effect of biochar amendments on the sorption and desorption herbicides in agricultural soil. In *Advanced Sorption Process Applications*; Edebali, S., Ed.; IntechOpen: London, UK, 2019; pp. 1–25.
17. Jensen, L.C.; Becerra, J.R.; Escudey, M. Impact of physical/chemical properties of volcanic ash-derived soils on mechanisms involved during sorption of ionisable and non-ionisable herbicides. In *Advanced Sorption Process Applications*; Edebali, S., Ed.; IntechOpen: London, UK, 2018; pp. 1–23.
18. Mielke, K.C.; Mendes, K.F.; Guimarães, T. Biochars effects on sorption and desorption of herbicides in soil. In *Interactions of Biochar and Herbicides in the Environment*; Mendes, K.F., Ed.; CRC Press: Boca Raton, FL, USA, 2022; pp. 131–157.
19. Trebst, A.; Wietoska, H. Mode of action and structure-activity-relationships of the aminotriazinone herbicide Metribuzin. Inhibition of photosynthetic electron transport in chloroplasts by Metribuzin. *Z. fur Nat. Sect. C Biosci.* **1975**, *30*, 499–504.
20. Saritha, J.D.; Ramprakash, T.; Rao, P.C.; Madhavi, M. Persistence of metribuzin in tomato growing soils and tomato fruits. *Nat. Environ. Pollut. Technol.* **2017**, *16*, 505.
21. Guimarães, A.C.D.; Mendes, K.F.; Campion, T.F.; Christoffoleti, P.J.; Tornisielo, V.L. Leaching of herbicides commonly applied to sugarcane in five agricultural soils. *Planta Daninha.* **2019**, *37*, e019181505. [CrossRef]
22. PPDB—Pesticide Properties Database. Footprint: Creating Tools for Pesticide Risk Assessment and Management in Europe. Developed by the Agriculture & Environment Research Unit (AERU), University of Hertfordshire, Funded by UK National Sources and the EU-funded FOOTPRINT Project (FP6-SSP-022704). Available online: <https://sitem.herts.ac.uk/aeru/ppdb/en/Reports/469.htm> (accessed on 10 March 2022).
23. Dores, E.F.G.C.; Navickiene, S.; Cunha, M.L.; Carbo, L.; Ribeiro, M.L.; De-Lamonica-Freire, E.M. Multiresidue determination of herbicides in environmental waters from Primavera do Leste Region (Middle West of Brazil) by SPE-GC-NPD. *J. Braz. Chem. Soc.* **2006**, *17*, 866–873. [CrossRef]
24. Kjær, J.; Olsen, P.; Henriksen, T.; Ullum, M. Leaching of metribuzin metabolites and the associated contamination of a sandy Danish aquifer. *Environ. Sci. Technol.* **2005**, *39*, 8374–8381. [CrossRef]
25. López-Piñeiro, A.; Peña, D.; Albarrán, A.; Becerra, D.; Sánchez-Llerena, J. Sorption, leaching and persistence of metribuzin in Mediterranean soils amended with olive mill waste of different degrees of organic matter maturity. *J. Environ. Manag.* **2013**, *122*, 76–84. [CrossRef] [PubMed]
26. Loffredo, E.; Parlavecchia, M.; Perri, G.; Gattullo, R. Comparative assessment of metribuzin sorption efficiency of biochar, hydrochar and vermicompost. *J. Environ. Sci. Health Part B* **2019**, *54*, 728–735. [CrossRef] [PubMed]
27. Mendes, K.F.; de Sousa, R.N.; Takeshita, V.; Alonso, F.G.; Régo, A.P.J.; Tornisielo, V.L. Cow bone char as a sorbent to increase sorption and decrease mobility of hexazinone, metribuzin, and quinclorac in soil. *Geoderma* **2019**, *343*, 40–49. [CrossRef]
28. Sigua, G.C.; Stone, K.C.; Hunt, P.G.; Cantrell, K.B.; Novak, J.M. Increasing biomass of winter wheat using sorghum biochars. *Agron. Sustain. Dev.* **2015**, *35*, 739–748. [CrossRef]
29. Jafri, N.; Wong, W.Y.; Doshi, V.; Yoon, L.W.; Cheah, K.H. A review on production and characterization of biochars for application in direct carbon fuel cells. *Process Saf. Environ. Prot.* **2018**, *118*, 152–166. [CrossRef]
30. Shaaban, M.; Van Zwieten, L.; Bashir, S.; Younas, A.; Núñez-Delgado, A.; Chhajro, M.A.; Kubar, K.A.; Ali, U.; Rana, M.S.; Mehmood, M.A.; et al. A concise review of biochar application to agricultural soils to improve soil conditions and fight pollution. *J. Environ. Manag.* **2018**, *228*, 429–440. [CrossRef]
31. Soares, M.B.; dos Santos, F.H.; Alleoni, L.R.F. Iron-modified biochar from sugarcane straw to remove arsenic and lead from contaminated water. *Water Air Soil Pollut.* **2021**, *232*, 1–13. [CrossRef]
32. Soares, M.B.; Milori, D.M.B.P.; Alleoni, L.R.F. How does the biochar of sugarcane straw pyrolysis temperature change arsenic and lead availabilities and the activity of the microorganisms in a contaminated sediment? *J. Soils Sediments* **2021**, *21*, 3185–3200. [CrossRef]
33. USEPA. *Method 3051A: Microwave Assisted Acid Digestion of Sediments, Sludges, Soils and Oils*; EPA: Washington, DC, USA, 2007.
34. Singh, B.; Camps-Arbestain, M.; Lehmann, J. *Biochar: A Guide to Analytical Methods*; CRC Press: Boca Raton, FL, USA, 2017.
35. Song, W.; Guo, M. Quality variations of poultry litter biochar generated at different pyrolysis temperatures. *J. Anal. Appl. Pyrolysis.* **2012**, *94*, 138–145. [CrossRef]

36. OECD—Organisation for Economic Co-Operation and Development. *Adsorption—Desorption Using a Batch Equilibrium Method*; OECD: Paris, France, 2000; 44p.
37. Mendes, K.F.; Sousa, R.N.; Soares, M.B.; Viana, D.G.; Souza, A.J. Sorption and desorption studies of herbicides in the soil by batch equilibrium and stirred flow methods. In *Radioisotopes in Weed Research*; Mendes, K.F., Ed.; CRC Press: Boca Raton, FL, USA, 2021; Volume 1, pp. 17–61.
38. Melo, L.C.; Coscione, A.R.; Abreu, C.A.; Puga, A.P.; Camargo, O.A. Influence of pyrolysis temperature on cadmium and zinc sorption capacity of sugar cane straw-derived biochar. *BioResources* **2013**, *8*, 4992–5004. [[CrossRef](#)]
39. Riaz, M.; Khan, M.; Ali, S.; Khan, M.D.; Ahmad, R.; Khan, M.J.; Rizwan, M. Sugarcane waste straw biochar and its effects on calcareous soil and agronomic traits of okra. *Arab. J. Geosci.* **2018**, *11*, 1–7. [[CrossRef](#)]
40. Ding, Y.; Liu, Y.; Liu, S.; Li, Z.; Tan, X.; Huang, X.; Zeng, G.; Zhou, L.; Zheng, B. Biochar to improve soil fertility. A review. *Agron. Sustain. Dev.* **2016**, *36*, 1–18. [[CrossRef](#)]
41. Tomczyk, A.; Sokołowska, Z.; Boguta, P. Biochar physicochemical properties: Pyrolysis temperature and feedstock kind effects. *Rev. Environ. Sci. Biotechnol.* **2020**, *19*, 191–215. [[CrossRef](#)]
42. Fidel, R.B.; Laird, D.A.; Thompson, M.L.; Lawrinenko, M. Characterization and quantification of biochar alkalinity. *Chemosphere* **2017**, *167*, 367–373. [[CrossRef](#)] [[PubMed](#)]
43. Novotny, E.H.; Maia, C.M.B.F.; Carvalho, M.T.M.; Madari, B.E. Biochar—Pyrogenic carbon for agricultural use—A critical review. *Rev. Bras. Cienc. Solo.* **2015**, *39*, 321–344. [[CrossRef](#)]
44. Zhao, S.X.; Ta, N.; Wang, X.D. Effect of temperature on the structural and physicochemical properties of biochar with apple tree branches as feedstock material. *Energies* **2017**, *10*, 1293. [[CrossRef](#)]
45. Farid, I.M.; Siam, H.S.; Abbas, M.H.; Mohamed, I.; Mahmoud, S.A.; Tolba, M.; Abbas, H.H.; Yang, X.; Antoniadis, V.; Rinklebe, J.; et al. Co-composted biochar derived from rice straw and sugarcane bagasse improved soil properties, carbon balance, and zucchini growth in a sandy soil: A trial for enhancing the health of low fertile arid soils. *Chemosphere* **2022**, *292*, e133389. [[CrossRef](#)]
46. Figueiredo, C.; Lopes, H.; Coser, T.; Vale, A.; Busato, J.; Aguiar, N.; Novotny, E.; Canellas, L. Influence of pyrolysis temperature on chemical and physical properties of biochar from sewage sludge. *Arch. Agron. Soil Sci.* **2018**, *64*, 881–889. [[CrossRef](#)]
47. Domingues, R.R.; Trugilho, P.F.; Silva, C.A.; Melo, I.C.N.D.; Melo, L.C.; Magriotis, Z.M.; Sanchez-Monedero, M.A. Properties of biochar derived from wood and high-nutrient biomasses with the aim of agronomic and environmental benefits. *PLoS ONE* **2017**, *12*, e0176884. [[CrossRef](#)]
48. Liu, Q.; Li, Y.; Chen, H.; Lu, J.; Yu, G.; Möslang, M.; Zhou, Y. Superior adsorption capacity of functionalised straw adsorbent for dyes and heavy-metal ions. *J. Hazard. Mater.* **2020**, *382*, 121040. [[CrossRef](#)]
49. Zhang, X.; Zhang, P.; Yuan, X.; Li, Y.; Han, L. Effect of pyrolysis temperature and correlation analysis on the yield and physicochemical properties of crop residue biochar. *Bioresour. Technol.* **2020**, *296*, 122318. [[CrossRef](#)]
50. Huang, F.; Zhang, S.M.; Wu, R.R.; Zhang, L.; Wang, P.; Xiao, R.B. Magnetic biochars have lower adsorption but higher separation effectiveness for Cd<sup>2+</sup> from aqueous solution compared to nonmagnetic biochars. *Environ. Pollut.* **2021**, *275*, 116485. [[CrossRef](#)]
51. Lopes, R.P.; Astruc, D. Biochar as a support for nanocatalysts and other reagents: Recent advances and applications. *Coord. Chem. Rev.* **2021**, *426*, 213585. [[CrossRef](#)]
52. Trivedi, M.; Branton, A.; Trivedi, D.; Nayak, G.; Singh, R.; Jana, S. Characterization of physical, spectral and thermal properties of biofield treated 1, 2, 4-Triazole. *Curr. Org. Chem.* **2015**, *3*, 1000128. [[CrossRef](#)]
53. Kamran, U.; Park, S.J. MnO<sub>2</sub>-decorated biochar composites of coconut shell and rice husk: An efficient lithium ions adsorption-desorption performance in aqueous media. *Chemosphere* **2020**, *260*, 127500. [[CrossRef](#)] [[PubMed](#)]
54. Chandra, S.; Bhattacharya, J. Influence of temperature and duration of pyrolysis on the property heterogeneity of rice straw biochar and optimization of pyrolysis conditions for its application in soils. *J. Clean. Prod.* **2019**, *215*, 1123–1139. [[CrossRef](#)]
55. Collard, F.X.; Blin, J. A review on pyrolysis of biomass constituents: Mechanisms and composition of the products obtained from the conversion of cellulose, hemicelluloses and lignin. *Renew. Sustain. Energy Rev.* **2014**, *38*, 594–608. [[CrossRef](#)]
56. Hassan, M.; Liu, Y.; Naidu, R.; Parikh, S.J.; Du, J.; Qi, F.; Willett, I.R. Influences of feedstock sources and pyrolysis temperature on the properties of biochar and functionality as adsorbents: A meta-analysis. *Sci. Total Environ.* **2020**, *744*, 140714. [[CrossRef](#)]
57. Wang, Y.; Jiang, B.; Wang, L.; Feng, Z.; Fan, H.; Sun, T. Hierarchically structured two-dimensional magnetic microporous biochar derived from hazelnut shell toward effective removal of p-arsanilic acid. *Appl. Surf. Sci.* **2021**, *540*, 148372. [[CrossRef](#)]
58. Silva, R.C.F.; Ardisson, J.D.; Cotta, A.A.C.; Araujo, M.H.; Carvalho, A.P.T. Use of iron mining tailings from dams for carbon nanotubes synthesis in fluidized bed for 17 $\alpha$ -ethinylestradiol removal. *Environ. Pollut.* **2020**, *260*, 114099. [[CrossRef](#)]
59. Huang, H.; Guo, T.; Wang, K.; Li, Y.; Zhang, G. Efficient activation of persulfate by a magnetic recyclable rape straw biochar catalyst for the degradation of tetracycline hydrochloride in water. *Sci. Total Environ.* **2021**, *758*, 143957. [[CrossRef](#)]
60. Sousa, R.N.; Soares, M.B.; Santos, F.H.; Leite, C.N.; Mendes, K.F. Interaction mechanisms between biochar and herbicides. In *Interactions of Biochar and Herbicides in the Environment*; Mendes, K.F., Ed.; CRC Press: Boca Raton, FL, USA, 2022; pp. 80–105.
61. Khalid, S.; Shahid, M.; Murtaza, B.; Bibi, I.; Naeem, M.A.; Niazi, N.K. A critical review of different factors governing the fate of pesticides in soil under biochar application. *Sci. Total Environ.* **2020**, *711*, 134645. [[CrossRef](#)]
62. Novak, J.M.; Busscher, W.J.; Laird, D.L.; Ahmedna, M.; Watts, D.W.; Niandou, M.A. Impact of biochar amendment on fertility of a southeastern coastal plain soil. *Soil Sci.* **2009**, *174*, 105–112. [[CrossRef](#)]

63. El-Naggar, A.; Lee, S.S.; Awad, Y.M.; Yang, X.; Ryu, C.; Rizwan, M.; Rinklebe, J.; Tsang, D.C.W.; Ok, Y.S. Influence of soil properties and feedstocks on biochar potential for carbon mineralization and improvement of infertile soils. *Geoderma* **2018**, *332*, 100–108. [[CrossRef](#)]
64. Oliveira, F.S.; Takeshita, V.; Mendes, K.F.; Tornisielo, V.L.; Alonso, F.G.; Junqueira, L.V.; Neto, M.B.; Lins, H.A.; Silva, D.V. Addition of raw feedstocks and biochars to the soil on the sorption–desorption and biodegradation of <sup>14</sup>C-saflufenacil. *Int. J. Environ. Sci. Technol.* **2022**, *1*, 1–18. [[CrossRef](#)]
65. Chintala, R.; Schumacher, T.E.; McDonald, L.M.; Clay, D.E.; Malo, D.D.; Papiernik, S.K.; Clay, S.A.; Julson, J.L. Phosphorus sorption and availability from biochars and soil/Biochar mixtures. *Clean—Soil Air Water* **2014**, *42*, 626–634. [[CrossRef](#)]
66. Glaser, B.; Lehr, V.I. Biochar effects on phosphorus availability in agricultural soils: A meta-analysis. *Sci. Rep.* **2019**, *9*, 1–9. [[CrossRef](#)]
67. Fernandes, J.D.; Chaves, L.H.G.; Dantas, E.R.B.; Tito, G.A.; Guerra, H.O.C. Phosphorus availability in soil incubated with biochar: Adsorption study. *Rev. Caatinga.* **2022**, *35*, 206–215. [[CrossRef](#)]
68. Hong, C.; Lu, S. Does biochar affect the availability and chemical fractionation of phosphate in soils? *Environ. Sci. Pollut. Res.* **2018**, *25*, 8725–8734. [[CrossRef](#)]
69. Naeem, M.A.; Khalid, M.; Aon, M.; Abbas, G.; Tahir, M.; Amjad, M.; Murtaza, B.; Yan, A.; Akhtar, S.S. Effect of wheat and rice straw biochar produced at different temperatures on maize growth and nutrient dynamics of a calcareous soil. *Arch. Agron. Soil Sci.* **2017**, *63*, 2048–2061. [[CrossRef](#)]
70. Jindo, K.; Audette, Y.; Higashikawa, F.S.; Silva, C.A.; Akashi, K.; Mastrolonardo, G.; Sánchez-Monedero, M.A.; Mondini, C. Role of biochar in promoting circular economy in the agriculture sector. Part 1: A review of the biochar roles in soil N, P and K cycles. *Chem. Biol. Technol. Agric.* **2020**, *7*, 1–12. [[CrossRef](#)]
71. Ippolito, J.A.; Spokas, K.A.; Novak, J.M.; Lentz, R.D.; Cantrell, K.B. Biochar elemental composition and factors influencing nutrient retention. In *Biochar for Environmental Management: Science, Technology and Implementation*; Lehmann, J., Stephen, J., Eds.; Routledge: New York, NY, USA, 2015; pp. 137–161.
72. Kongthod, T.; Thanachit, S.; Anusontpornperm, S.; Wiriyakitnateekul, W. Effects of biochars and other organic soil amendments on plant nutrient availability in an ustoxic quartzipsamment. *Pedosphere* **2015**, *25*, 790–798. [[CrossRef](#)]
73. Ippolito, J.A.; Stromberger, M.E.; Lentz, R.D.; Dungan, R.S. Hardwood biochar influences calcareous soil physicochemical and microbiological status. *J. Environ. Manag.* **2014**, *43*, 681–689. [[CrossRef](#)]
74. Li, S.; Barreto, V.; Li, R.; Chen, G.; Hsieh, Y.P. Nitrogen retention of biochar derived from different feedstocks at variable pyrolysis temperatures. *J. Anal. Appl. Pyrolysis.* **2018**, *133*, 136–146. [[CrossRef](#)]
75. Hailegnaw, N.S.; Mercl, F.; Pračke, K.; Száková, J.; Tlustoš, P. Mutual relationships of biochar and soil pH, CEC, and exchangeable base cations in a model laboratory experiment. *J. Soils Sediments* **2019**, *19*, 2405–2416. [[CrossRef](#)]
76. Da Silva Mendes, J.; Fernandes, J.D.; Chaves, L.H.G.; Guerra, H.O.C.; Tito, G.A.; de Brito Chaves, I. Chemical and physical changes of soil amended with biochar. *Water Air Soil Pollut.* **2021**, *232*, 1–13. [[CrossRef](#)]
77. Limousin, G.; Gaudet, J.P.; Charlet, L.; Szenknect, S.; Barthes, V.; Krimissa, M. Sorption isotherms: A review on physical bases, modeling and measurement. *Appl. Geochem.* **2007**, *22*, 249–275. [[CrossRef](#)]
78. Rigi, M.R.; Farahbakhsh, M.; Rezaei, K. Adsorption and desorption behavior of herbicide metribuzin in different soils of Iran. *J. Agric. Sci. Technol.* **2015**, *17*, 777–787.
79. Peña, D.; López-Piñeiro, A.; Albarrán, Á.; Rato-Nunes, J.M.; Sánchez-Llerena, J.; Becerra, D.; Ramírez, M. De-oiled two-phase olive mill waste may reduce water contamination by metribuzin. *Sci. Total Environ.* **2016**, *541*, 638–645. [[CrossRef](#)] [[PubMed](#)]
80. Saritha, J.D.; Prakash, T.R.; Madhavi, M.; Rao, P.C. Adsorption of metribuzin in tomato growing soils. *Int. J. Chem. Stud.* **2017**, *5*, 740–746.
81. Downie, A.; Crosky, A.; Munroe, P. Physical properties of Biochar. In *Biochar for Environmental Management, Science and Technology*; Lehmann, J.L., Joseph, S., Eds.; Earthscan: London, UK, 2009; pp. 13–32.
82. White, P.M., Jr.; Potter, T.L.; Lima, I.M. Sugarcane and pinewood biochar effects on activity and aerobic soil dissipation of metribuzin and pendimethalin. *Ind. Crops Prod.* **2015**, *74*, 737–744. [[CrossRef](#)]
83. Gámiz, B.; Hall, K.; Spokas, K.A.; Cox, L. Understanding activation effects on low-temperature biochar for optimization of herbicide sorption. *Agronomy* **2019**, *9*, 588. [[CrossRef](#)]
84. Keiluweit, M.; Nico, P.S.; Johnson, M.G.; Kleber, M. Dynamic molecular structure of plant biomass-derived black carbon (biochar). *Environ. Sci. Technol.* **2010**, *44*, 1247–1253. [[CrossRef](#)]
85. Xiao, F.; Pignatello, J.J.  $\pi^+ - \pi$  Interactions between (Hetero) aromatic Amine cations and the graphitic surfaces of pyrogenic carbonaceous materials. *Environ. Sci. Technol.* **2015**, *49*, 906–914. [[CrossRef](#)] [[PubMed](#)]
86. Cara, I.G.; Filip, M.; Bulgariu, L.; Raus, L.; Topa, D.; Jitareanu, G. Environmental remediation of metribuzin herbicide by mesoporous carbon-rich from wheat straw. *Appl. Sci.* **2021**, *11*, 4935. [[CrossRef](#)]
87. Kah, M.; Sigmund, G.; Xiao, F.; Hofmann, T. Sorption of ionizable and ionic organic compounds to biochar, activated carbon and other carbonaceous materials. *Water Res.* **2017**, *124*, 673–692. [[CrossRef](#)]
88. Wei, L.; Huang, Y.; Li, Y.; Huang, L.; Mar, N.N.; Huang, Q.; Liu, Z. Biochar characteristics produced from rice husks and their sorption properties for the acetanilide herbicide metolachlor. *Environ. Sci. Pollut. Res.* **2017**, *24*, 4552–4561. [[CrossRef](#)]

89. Liu, K.; He, Y.; Xu, S.; Hu, L.; Luo, K.; Liu, X.; Liu, M.; Zhou, X.; Bai, L. Mechanism of the effect of pH and biochar on the phytotoxicity of the weak acid herbicides imazethapyr and 2,4-D in soil to rice (*Oryza sativa*) and estimation by chemical methods. *Ecotoxicol. Environ. Saf.* **2018**, *161*, 602–609. [[CrossRef](#)]
90. Delgado-Moreno, L.; Almendros, G.; Peña, A. Raw or incubated olive-mill wastes and its biotransformed products as agricultural soil amendments e effect on sorption e desorption of triazine herbicides. *J. Agric. Food Chem.* **2007**, *55*, 836e843. [[CrossRef](#)]
91. Majumdar, K.; Singh, N. Effect of soil amendments on sorption and mobility of metribuzin in soils. *Chemosphere* **2007**, *66*, 630e637. [[CrossRef](#)]
92. Mendes, K.F.; Furtado, I.F.; Sousa, R.N.D.; Lima, A.D.C.; Mielke, K.C.; Brochado, M.G.D.S. Cow bonechar decreases indaziflam pre-emergence herbicidal activity in tropical soil. *J. Environ. Sci. Health Part B* **2021**, *56*, 532–539. [[CrossRef](#)]
93. Lian, F.; Xing, B. Black carbon (biochar) in water/soil environments: Molecular structure, sorption, stability, and potential risk. *Environ. Sci. Technol.* **2017**, *51*, 13517–13532. [[CrossRef](#)]
94. Barriuso, E.; Laird, D.A.; Koskinen, W.C.; Dowdy, R.H. Atrazine desorption from smectites. *Soil Sci. Soc. Am. J.* **1994**, *58*, 1632–1638. [[CrossRef](#)]
95. Singh, N.; Raunaq; Singh, S.B. Effect of fly ash on sorption behavior of metribuzin in agricultural soils. *J. Environ. Sci. Health Part B* **2012**, *47*, 89–98. [[CrossRef](#)]
96. Yu, X.Y.; Ying, G.G.; Kookana, R.S. Sorption and desorption behaviors of diuron in soils amended with charcoal. *J. Agric. Food Chem.* **2006**, *54*, 8545–8550. [[CrossRef](#)]
97. Deng, H.; Feng, D.; He, J.X.; Li, F.Z.; Yu, H.M.; Ge, C.J. Influence of biochar amendments to soil on the mobility of atrazine using sorption-desorption and soil thin-layer chromatography. *Ecol. Eng.* **2017**, *99*, 381–390. [[CrossRef](#)]
98. Liu, Y. Is the free energy change of adsorption correctly calculated? *J. Chem. Eng. Data* **2009**, *54*, 1981–1985. [[CrossRef](#)]
99. Carter, M.C.; Kilduff, J.E.; Weber, W.J. Site energy distribution analysis of preloaded adsorbents. *Environ. Sci. Technol.* **1995**, *29*, 1773–1780. [[CrossRef](#)]
100. Gisi, S.; Lofrano, G.; Grassi, M.; Notarnicola, M. Characteristics and adsorption capacities of low-cost sorbents for wastewater treatment: A review. *Sustain. Mater. Technol.* **2016**, *9*, 10–40. [[CrossRef](#)]